Environmental Science Nano

ROYAL SOCIETY OF CHEMISTRY

PAPER

View Article Online
View Journal | View Issue

Cite this: *Environ. Sci.: Nano*, 2025, **12**, 1230

Mechanistic insights into the adsorption of different types of VOCs on monolayer MoS_2 *via* first-principles approaches†

Weina Zhao, [ab] Jinlong Wang,[ab] Chang Shen,[ab] Bufan Xie,[ab] Guiying Li [ab] and Taicheng An *[ab]

Emissions from industrial activities have led to the significant accumulation of volatile organic compounds (VOCs) in the atmosphere, raising substantial concerns due to their serious threats to human health and the global environment in recent years. Among the various strategies for VOC abatement, adsorption technology has emerged as a promising approach for effectively removing VOCs from contaminated air. However, the adsorption behavior and mechanisms for different VOC species remain poorly understood. Herein, the adsorption characteristics of eight typical VOC categories (C ≤ 8 atoms) commonly emitted by the petrochemical industry were systematically investigated using density functional theory (DFT) calculations at the electronic and atomic levels on monolayer MoS_2. The VOC categories analyzed include alkanes, alkenes, alkynes, alcohols, aldehydes, carboxylic acids, ketones and aromatic hydrocarbons. Our research was aimed at investigating the adsorption behaviors of various types of VOCs, including those with varying carbon chain lengths within the same category. Results demonstrated that the unique structural properties of the MoS_2 monolayer not only provided excellent adsorption capabilities but also exhibited distinct responses to the eight aforementioned VOC categories. The adsorption energies of the VOCs followed a distinct hierarchical order, alkanes < aromatic hydrocarbons < alkynes < aldehydes < ketones < alkenes < alcohols < carboxylic acids, with the values ranging from −0.25 to −1.19 eV. In different VOC adsorption systems, the distance between the rightmost peak of the density of states (DOS) and the Fermi level ranged from −1.42 to −0.17 eV. Additionally, for a given VOC category, it was observed that an increase in carbon chain length correlated with an increase in adsorption energy. A predictive fitting curve for the adsorption energy of VOCs was derived and expressed as E_{ads} (E_v) = −0.13X − 0.12, where X represents the number of carbon atoms. Through comprehensive analyses involving charge density differences, DOS and Mulliken charge analysis, the underlying mechanisms correlating adsorption energy with both VOC species and carbon chain length were elucidated. Our research highlights the potential of MoS_2 as a promising candidate for selective VOC adsorption and provides a theoretical framework for the development of high-performance VOC adsorbents.

Received 10th October 2024,
Accepted 14th December 2024

DOI: 10.1039/d4en00953c

rsc.li/es-nano

Environmental significance

The release of volatile organic compounds (VOCs) from industrial activities poses significant environmental and health risks, prompting the development of effective abatement strategies. Among these, adsorption is recognized as a promising technique for VOC removal from contaminated air. However, a comprehensive understanding of the adsorption mechanisms and the varying trends across different VOC species remains insufficient. Herein, we developed and examined adsorption models for eight distinct VOC types on monolayer MoS_2 at both the electronic and atomic levels. Our findings showed that MoS_2 interacted uniquely with each VOC category, and adsorption energy significantly increased with the increase in carbon chain length within the same category. We elucidated the fundamental relationship between adsorption energy, electronic structure, and VOC category, thereby facilitating advancements in the development of high-performance adsorption applications.

[a] *Guangdong Key Laboratory of Environmental Catalysis and Health Risk Control, Guangdong Hong Kong-Macao Joint Laboratory for Contaminants Exposure and Health, Institute of Environmental Health and Pollution Control, Guangdong University of Technology, Guangzhou 510006, China. E-mail: antc99@gdut.edu.cn*
[b] *Guangdong Engineering Technology Research Center for Photocatalytic Technology Integration and Equipment, Guangzhou Key Laboratory of Environmental Catalysis and Pollution Control, School of Environmental Science and Engineering, Guangdong University of Technology, Guangzhou 510006, China*

† Electronic supplementary information (ESI) available. See DOI: https://doi.org/10.1039/d4en00953c

1. Introduction

In recent years, increasing attention has been directed toward the environmental pollution caused by volatile organic compounds (VOCs) emitted into the atmosphere from industrial activities. These pollutants pose serious threats not only to human health, leading to headaches, lung cancer and even death, but also to the global environment and climatic conditions.[1–5] In addition, VOCs serve as precursors for the formation of atmospheric contaminants,[6–8] such as tropospheric ozone, photochemical smog and secondary organic aerosols (SOAs). More concerning is the dramatic increase in annual industrial VOC emissions in recent years, particularly in the developing world. Due to the severe adverse effects of VOCs and the growing awareness of the need to strengthen efforts to combat air pollution, governments worldwide have promulgated increasingly stringent emission standards to limit VOCs emitted from various industrial processes. Under China's 14th Five-Year Plan (2020–2025), the total VOC emissions are targeted to be reduced by more than 10%. Therefore, the advancement of practical technologies aimed at reducing VOC emissions and effectively eliminating VOCs should be a paramount priority within the domain of environmental protection.

Among the available VOC abatement options,[6] adsorption and catalytic oxidation are two types of promising VOC removal technologies in industries.[9–14] However, due to the complicated industrial VOC emission characteristics, catalytic oxidation is mainly limited to the catalytic conversion of VOCs to CO_2 and H_2O, which violates the carbon peaking and carbon neutrality targets.[15] Owing to the advantages of being a low-cost and facile operation with high efficiency of adsorbents, in contrast, the selective adsorption-based technologies[16,17] have been widely considered as one of the mainstream routes for VOC abatement that facilitates the recovery of products with substantial added value for the high concentration, while the removal of VOCs at low-to-medium concentration ($<$1000 mg m^{-3}) can also be effectively achieved. Thus, the selection of adsorbent in an effective adsorption process is undoubtedly important.

A new family of two-dimensional (2D) materials, including graphene,[18] boron-nitride (h-BN)[19] and the transition metal dichalcogenide structures (TMDs), has been developed and are promising candidates for VOC adsorption, owing to the appropriate textural properties (surface area and pore geometry, *etc.*) and surface physicochemical properties. Among them, monolayer MoS_2 has been intensely studied,[20,21] and shown the feasibility of high-throughput production from the earth-abundant natural molybdenite mineral. As one of the novel 2D honeycomb semiconductors with a direct band gap of 1.9 eV,[22] the MoS_2 monolayer is composed of three atomic layers (S–Mo–S) with hexagonal symmetry, while these monolayers are stacked on top of each other by weak van der Waals interactions. Specifically, many studies demonstrate that the MoS_2 monolayer shows great gas-sensing performance[23] with high adsorption capacity, owing to the high specific surface area, semiconducting properties and huge active sites. For example, to exploit the gas-sensing capabilities of MoS_2, Xue's group[24] studied the adsorption of various gas molecules, including CO, CO_2, NH_3, NO, NO_2, CH_4, H_2O, N_2, O_2 and SO_2, on the MoS_2 monolayer *via* first-principle calculations. They find that MoS_2 shows more sensitivity towards NO, NO_2 and SO_2 gases. Similarly, Shokri *et al.*[25] also investigated the adsorption of various gas molecules (H_2, O_2, H_2O, NH_3, NO, NO_2, CO and CO_2) to explore the sensing capabilities of monolayer MoS_2, and revealed distinct variations in the adsorption capacities of these molecules on the MoS_2 surface. Nagarajan *et al.*[26] reported on the electronic and adsorption properties of three different alcohol molecules, namely methanol, ethanol and 1-propanol vapors on the monolayer MoS_2 nanosheet, and confirmed that the adsorption of the 1-propanol molecule is the most favorable rather than methanol or ethanol vapors. Yakobson *et al.* mainly concentrated on the theoretical comprehension of the adsorption behavior of various types of VOCs on monolayer MoS_2 and its underlying mechanism, with a focus on offering a comprehensive analysis of the adsorption trends and mechanisms.[27]

Furthermore, some researchers found that transition-metal decorated systems can be used to improve the sensitivity of monolayer MoS_2 to VOCs (including ethanol, acetone, propanal or formaldehyde) and small gas molecules.[28] Liu *et al.* have demonstrated that the photocatalytic activity of MoS_2 is significantly enhanced through metal ion doping (*e.g.*, Ag, Cu), enabling the effective degradation of organic pollutants under visible light irradiation.[29–32] Wang *et al.* discovered that after the combination of the MoS_2 composite material with other functional materials, the removal effect of VOCs is significantly improved, and it has good stability and reusability.[33] Chen *et al.* designed a MoS_2-based sensor that can selectively detect VOCs at room temperature through interface engineering. The optimized sensor exhibited excellent sensitivity and anti-interference ability to benzene, toluene, and other VOCs.[34] Zhao *et al.*[35] focused on enhancing the adsorption performance of MoS_2 through Group VIII transition metal doping, and explored the electronic properties and charge transfer mechanisms in detail. A number of different ideas and methods have been put forward to explore MoS_2 materials. Density functional theory calculations have also shown that the electronic structure of the monolayer adsorbent MoS_2 doped with metal atoms is significantly altered upon gas adsorption, which then has an effect on the formation of covalent bonds between them. According to the above studies, it is evident that the monolayer MoS_2 can be efficiently used as the adsorption substrate of inorganic small molecules and VOC molecules.

Although some studies on the adsorption of VOC molecules on monolayer MoS_2 have been reported, many efforts have focused on improving the adsorption capacity of monolayer MoS_2 *via* doping transition metal atoms, and little is known about the adsorption capability variety of different types of VOC molecules. Therefore, in this work, the adsorption

mechanism of eight typical types of VOCs (C ≤ 8 atoms) discharged from the petrochemical industry on the MoS_2 monolayer were systematically studied *via* first-principles calculations based on DFT. The VOCs included alkanes, alkenes, alkynes, alcohols, aldehydes, carboxylic acids, ketones, and aromatic hydrocarbons. The calculated adsorption energies with different orientations of VOC molecules were exploited to establish the most favorable adsorption models for the VOCs–MoS_2 interaction. By optimizing the geometrical structure, computing the adsorption energy, analysing the density of states (DOS), charge density differences and Mulliken charge analysis, we found an obvious adsorption regularity for different types of VOCs with different carbon chain lengths on MoS_2, and provided general guidance for various types of VOC removal in industrial production.

2. Calculation methods

All of the spin calculations in this work were performed based on DFT *via* Dmol3 module in Material Studio software.[36] The general gradient approximation with Perdew–Burke–Ernzerh function (GGA-PBE) was adopted to describe the exchange-correlation interactions.[37] A van der Waals (vdW) correction was incorporated *via* the DFT+D method within the Tkatchenko-Scheffler (TS) to describe the weak interactions in all calculations.[38] Double numerical plus polarization (DNP) was adopted as the basic set, and the interactions between the core ions and electrons were employed by utilizing OTFG-ultrasoft pseudopotentials.[39] A smearing of 0.005 Ha was employed to accelerate the structure convergence. The convergence tolerance of energy for geometry optimization was set to 10^{-5} Hartree (1 Hartree = 27.21 eV), while the maximum allowed force and displacement were 0.002 Hartree and 0.005 Å, respectively.

The monolayer MoS_2 used in our simulation consists of a 4 × 4 × 1 periodic supercell with a vacuum width of 30 Å along the *Z*-axis, which ensures that the interaction between two adjacent supercells is negligible. All atoms were allowed to relax together with the adsorbate for geometry optimization, and the optimized parameters are consistent with those previously reported.[40] The Brillouin zone was sampled with a Monkhorst–Pack mesh of 5 × 5 × 1 *k*-points in the reciprocal space. It should be noted that the VOC molecules were initially placed above the MoS_2 substrate with a distance of about 2.5 A to ensure that the VOC molecules bind to the substrate from all possible spatial orientations. The adsorption energy E_{ads} of the VOC molecules on the monolayer MoS_2 is defined as:

$$E_{ads} = E_{MoS_2+VOCs} - E_{MoS_2} - E_{VOCs} \quad (1)$$

where E_{MoS_2+VOCs}, E_{MoS_2}, and E_{VOCs} are the total energies of the system for the VOC molecule absorbed on MoS_2, the isolate monolayer MoS_2, and a free VOC molecule, respectively.

Desorption performance is one of the important indicators to measure the adsorption capacity of the adsorbents. Studying the effect of the surface modification of MoS_2 on the analytical performance can more comprehensively evaluate its performance as an adsorbent.[41–43] The resolution time T of VOC molecules on a single layer of molybdenum disulfide is defined as:

$$T = A^{-1} \exp(-E_a/K_B T_1) \quad (2)$$

where A stands for the attempt frequency and the unit is (10^{12} s^{-1}), E_a stands for the adsorption energy E_{ads}, K_B stands for the Boltzmann constant (8.62 × 10^{-5} eV K^{-1}), and T_1 stands for Kelvin temperature, which is taken as 298 K in this calculation.

3. Results and discussion

3.1 Geometries and interfacial adsorption behaviors of the monolayer MoS_2

The bulk 2H-MoS_2 unit cell used in this work contained six atoms with an in-plane lattice constant a (= b) and an out-of-plane lattice constant c, as shown in Fig. S1.† It belongs to the hexagonal structure, while the DFT optimized lattice parameters are (a = b = 3.22 Å) for the 2H-MoS_2 crystal, which agrees well with the experimental lattice (a = b = 3.16 Å,[24] c = 12.30 Å, and the angles (degrees) α = β = 90°, γ = 120° in lattice constants). The MoS_2 monolayer consists of three covalently bonded hexagonal atomic sheets (S–Mo–S) with the Mo atom in the sublayer sandwiched between two S atom layers outside in the 2H phase by the stacking order of ABA, while each monolayer is stacked together by weak van der Waals interactions. The single-layered MoS_2 consists of three atomic layers with a space group of (D_{3h}) $P6/m2$ (187). For the optimized monolayer structure, the S–Mo–S angle is 80.5° and the bond distance of S–Mo is 2.45 Å, which is longer by 0.04 Å than that of the experiment value,[24] as shown in Fig. 1a.

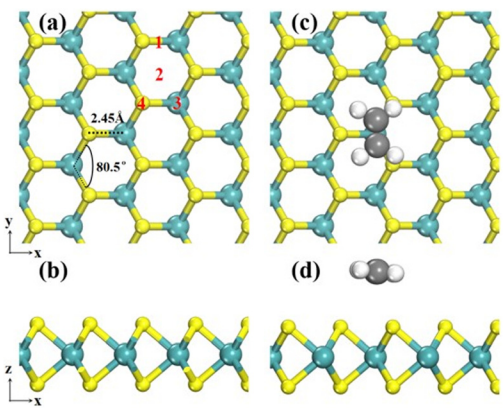

Fig. 1 Top and side views of the optimized geometries of the (a and b) pristine and (c and d) ethylene-adsorbed MoS_2 monolayer, respectively. Bond lengths in Å. The red numbers in the figure represent the possible adsorption sites on the MoS_2 surface. The yellow, cyan, gray and white spheres represent the S, Mo, C and H atoms herein and in the following figures, respectively.

The high specific surface area of MoS_2, which provides not only more adsorption sites for gas molecules but also additional active sites for surface modification, has accelerated the development of MoS_2 as a promising adsorption substrate. Thus, it is of great importance to gain an in-depth understanding of the surface structural characteristics, which is related to the adsorption behavior.[44] Based on the above depicted surface models, herein, all four typical high-symmetry surface decorating sites marked by red numbers in Fig. 1a are taken into account; namely, the bridge site (1, above the midpoint between nearest-neighbor S and Mo atoms), hollow site (2, above the center of hexagon), top site above Mo atoms (3), and top site above the S atoms (4). In order to better understand the surface adsorption sites, we first take ethylene as an example to describe its adsorption behavior. The most favorable configuration of ethylene on the MoS_2 monolayer (*cf.* Fig. 1b) is obtained from several possible structural candidates. Through the structure optimization and adsorption energy calculations, our results showed that ethylene was adsorbed at the top site above the Mo atoms (site 3) with an adsorption energy of −0.37 eV, while the preferred adsorption structure exhibits a carbon chain parallel to the MoS_2 substrate with a vertical distance of 3.72 Å, as shown in Fig. 1b.

3.2 Adsorption of different types of VOCs on monolayer MoS_2

To provide insights into the adsorption behavior of different types of VOC molecules, the adsorptions of eight types of typical VOC molecules (*e.g.*, alkanes, alkenes, alkynes, alcohols, aldehydes, carboxylic acids, ketones and aromatic hydrocarbons) with the number of C ≤ 8 atoms on MoS_2 monolayer were considered. In this work, the DFT+D method within the OBS scheme is adopted to deal with the vdW interactions[45] for the low-dimensional adsorption systems. In order to more clearly compare the adsorption behavior of different VOC molecules, we first determined the optimized adsorption configuration with seven carbon atoms, as shown in Fig. 2. To obtain the most favorable adsorption configuration, based on the four adsorption sites labeled in red in Fig. 1a, the VOC molecules were initially placed at all possible sites with different orientations on the MoS_2 monolayer.

The optimized configurations of the adsorbed VOC molecules on the MoS_2 monolayer with seven carbon atoms are displayed in Fig. 2, which correspond to heptane, toluene, heptyne, heptaldehyde, heptanone, heptylene, heptyl alcohol and heptanoic acid. For the adsorption configurations, it showed that all eight VOC molecules were parallel to the MoS_2 surface by zigzag chain structures, with the vertical distances between the carbon chain and substrate at 3.73, 3.55, 3.58, 3.58, 3.56, 3.59, 3.68, and 3.54 Å, respectively. The interaction between the VOC molecules and MoS_2 monolayer can be discerned through analyses of the adsorption energy and charge transfer. However, the distance between the VOCs and MoS_2 may be slightly greater, which is potentially attributable to the steric hindrance that is present. Therefore, the strong adsorption may partly come from the slight structural deformation of MoS_2 and partially from the dramatic deformation of VOCs. In addition, there were some changes of C–C, C–H and C═O bond distance in the VOC molecules after adsorption, but all is less than 0.1 Å, indicating no occurrence of spontaneous decomposition of VOC molecules on the MoS_2 monolayer.

Next, we calculated the corresponding adsorption energy of heptane, toluene, heptyne, heptaldehyde, heptanone, heptylene, heptyl alcohol and heptanoic acid on the MoS_2 monolayer, as listed in Table 1. The negative adsorption energy signifies an exothermic adsorption process.[18] Among these VOCs, the adsorption energies spanned from −0.98 to −1.08 eV, which is within the range of strong chemisorption, indicating that the MoS_2 monolayer has very good adsorption properties for various types of VOCs with seven carbons. Additionally, for a given VOC molecule, there was a correlation between the charge transfer amount and the adsorption energy, *i.e.*, when the adsorption energy is stronger, normally more electrons are transferred between the MoS_2 substrate and VOC molecules, as listed in Table 1. For example, toluene possessed an adsorption energy of −0.99 eV with a smaller charge transfer of 0.079 e, which may be due to the steric-hindrance effect of the benzene ring. It can also be seen that the unsaturated bond C═C/C≡C or C–

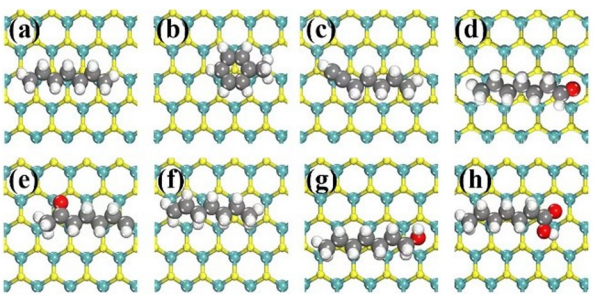

Fig. 2 Optimized structures of thermodynamically preferred models of different VOCs with seven C atoms on the MoS_2 monolayer. (a)–(h) are the corresponding heptane, toluene, heptyne, heptaldehyde, heptanone, heptylene, heptyl alcohol and heptanoic acid, respectively. The red sphere in this and the following figures is the O atom.

Table 1 Calculated adsorption energies, electron transfer amount and desorption time of the adsorbed heptane, toluene, heptyne, heptaldehyde, heptanone, heptylene, heptyl alcohol and heptanoic acid on the monolayer MoS_2. Q_v is the amount of electron transfer of the adsorbed VOC molecules after adsorption. τ represents the desorption time of the adsorbed VOC molecules

Types	E_{ads} (eV)	Q_v (e)	τ (s)
$CH_3(CH_2)_5CH_3$	−0.98	0.078	3.70×10^4
$C_6H_5CH_3$	−0.99	0.079	5.47×10^4
$CH{\equiv}C(CH_2)_4CH_3$	−1.00	0.081	8.07×10^4
$CH_3(CH_2)_5CHO$	−1.03	0.083	2.60×10^5
$CH_3CO(CH_2)_4CH_3$	−1.03	0.083	2.60×10^5
$CH_2{=}CH(CH_2)_4CH_3$	−1.04	0.088	3.83×10^5
$CH_3(CH_2)_6OH$	−1.07	0.089	1.23×10^6
$CH_3(CH_2)_5COOH$	−1.08	0.091	1.82×10^6

O/C═O in VOC molecules can increase the charge transfer between the substrate and VOCs.

To further understand the adsorption variability mechanism of the different types of VOCs, we calculated the total projected density of states (DOS) of the adsorbed VOCs on the MoS_2 monolayer, as shown in Fig. 3. The electronic structure is an intrinsic factor toward understanding the adsorption behavior,[13] and is thus important in the adsorption process. After adsorption, there was an obvious difference in the electronic structure of the VOC/MoS_2 adsorption system *vis-à-vis* the original perfect substrate. With respect to the valence band maximum (VBM) of the pure MoS_2 (*cf.* Fig. S2†), the VBM of the VOC/MoS_2 systems gradually moved left, directly indicating that the VOC molecules lose electrons after adsorption. For the different VOC adsorption systems, the distance between the rightmost peak of DOS and the Fermi energy level was from −1.42 to −0.17 eV with the corresponding order: heptane > toluene > heptyne > heptaldehyde > heptanone > heptylene > heptyl alcohol > heptanoic acid. Fig. 3 shows that if DOS moves towards negative energy near the Fermi level, the adsorption behavior of X will adjust the electron energy states of the whole system so that VOC molecules are more favorable for binding to the substrate, which is in agreement with the adsorption energy for the different types of VOCs described above. The DOS analysis has been extensively documented in previous literature to elucidate the adsorptive properties of gas molecules.[14] Basically, there is a stronger interaction between the VOCs and MoS_2 substrate as DOS approaches the Fermi energy level. This may be the main cause for the gradual left shift of the DOS peak for the different types of VOCs near the Fermi level. From the above, it can be seen that the adsorption of different VOC species was sensitive to the MoS_2 monolayers, which was beneficial for the specific VOC removal.

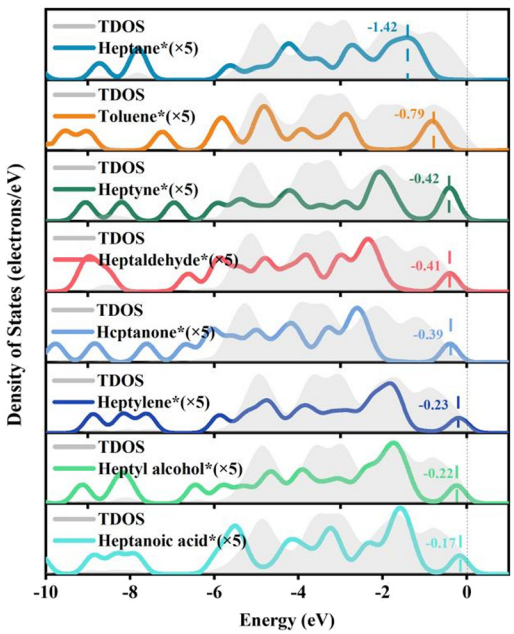

Fig. 3 The total and projected density of states for 8 typical VOC molecules (having 7 carbon atoms) adsorbed on a single layer of MoS_2. The Fermi level is set to zero.

3.3 Adsorption of the same VOC category with different carbon-chain lengths on monolayer MoS_2

In order to systematically explore the effect of the carbon chain lengths on VOC adsorption, the adsorption behavior of VOC molecules of the same kind with different carbon chain lengths (C ≤ 8 atoms) on the MoS_2 monolayer was further investigated. For simplicity, herein we took alkanes (2 ≤ C ≤ 8 atoms) as an example to illustrate the effect of carbon chains on VOC adsorption. After configuration optimization, the most favorable adsorption geometries and local adsorption geometries of VOC molecules on the MoS_2 monolayer were obtained, and are shown in Fig. 4. We can clearly see that the alkanes of C2–C8 are adsorbed nearly parallel on the MoS_2 surface to form a stable adsorption configuration. It is worth noting that there was no covalent bond in the interface area, inferring that the electron saturation of the H atom in VOCs hinders bond formation. Next, we calculated the adsorption energy of alkanes on MoS_2. The corresponding adsorption energies of CH_3CH_3, $CH_3CH_2CH_3$, $CH_3(CH_2)_2CH_3$, $CH_3(CH_2)_3CH_3$, $CH_3(CH_2)_4CH_3$, $CH_3(CH_2)_5CH_3$ and $CH_3(CH_2)_6CH_3$ were −0.34, −0.49, −0.62, −0.76, −0.88, −0.98, and −1.14 eV, respectively. Of particular interest is that the adsorption energies of VOCs of the same type increased significantly with the increase of the carbon chain length. To understand why, we performed a series of electronic structure calculations, as described below.

In Fig. 5, we show the calculated charge density differences (CDD) diagram of the corresponding adsorption system along the MoS_2 (0 0 1) axis in the unit of e. The charge density diagram can show the accumulation of electron density during the VOC adsorption.[46] According to our results, the isosurface plane of the CDD in Fig. 5 was exactly parallel to the VOC molecule, and then passed through each C atom. Blue indicates the electrons captured, red indicates the electrons lost, while the green part is the area of the vacuum layer. The charge distribution around the C and H atoms indicates the covalent characteristics by C–H bonds in the VOC molecules,

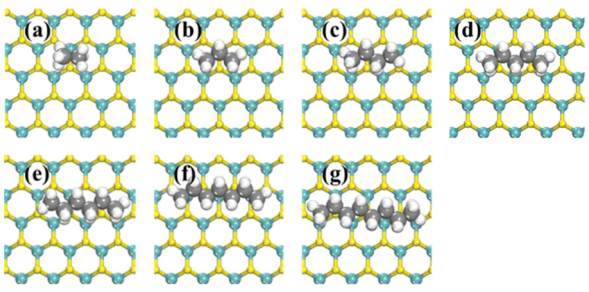

Fig. 4 Optimized structures of thermodynamically preferred models for alkanes with different carbon chains on monolayer MoS_2. (a)–(g) are the corresponding alkanes with the carbon number from C2 to C8 molecules, respectively.

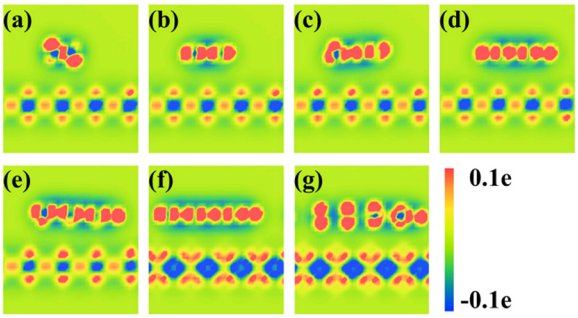

Fig. 5 Isosurface of the charge density difference for alkanes with varying carbon chain lengths on monolayer MoS_2. (a)–(g) Correspond to alkanes with carbon numbers ranging from C2 to C8, respectively. Electron accumulation and depletion areas are represented by blue and red, respectively. The green region represents the vacuum layer area.

while there is a higher accumulation of the electron density in the H atom. Thus, after adsorption, electrons will be transferred from alkanes to the MoS_2 surface, which is similar to that observed from Liu' studies for benzene adsorption on MoS_2 *via* CDD analysis.[47] Obviously, charge transfer between VOCs and the MoS_2 substrate plays a major role during the adsorption process. This indicates a corresponding adsorption variation of importance, wherein the area of electron loss region from the VOC molecules increases with the increase of the carbon chain length, *i.e.*, the long carbon chain has a stronger electronic interaction effect than the short carbon chain on MoS_2.

Then, the Mulliken charge analysis of the alkane molecules on the MoS_2 monolayer was also investigated, as shown in Fig. 6. Mulliken charge analysis elucidates that there is a small amount of charge transfer from the alkane molecules to the substrate in the adsorption system. This is probably mainly because each C atom of an alkane is saturated with H atoms, which will prevent other chemical bond formations by affecting the amount of charge transfer corresponding to the benzene adsorption process.[48] Generally, the large charge transfer on the adsorption system reflects the higher adsorption energy. It is of importance that

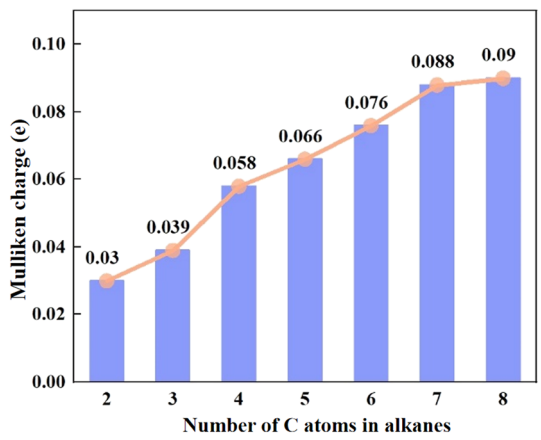

Fig. 6 Mulliken charge diagram of the adsorbed alkanes with varying carbon chain lengths on monolayer MoS_2.

the Mulliken charge amount transferred from the alkanes to MoS_2 gradually increased with the increase of the carbon chain length, with the maximum of 0.08 e for heptane adsorption, as shown in Table 1. This indicates that each carbon atom in the alkanes can provide electrons to the substrate with the change of the molecular morphology from neutral to cationic, which facilitates the interaction between VOCs and the substrate, and elucidates the observed trend of increasing adsorption energy concomitant with the elongation of the carbon chain.

In addition, the electronic density distribution of alkane molecules with carbon numbers ranging from 2–8 adsorbed on the MoS_2 substrate was calculated, and is shown in Fig. 7. After adsorption, the seven density bands of the adsorption system also moved downward *vis-à-vis* the original perfect MoS_2 substrate. This indicates that the electrons are transferred from the alkanes to the substrate surface, which is in good agreement with the Mulliken charge analysis discussed previously. Moreover, it obviously shows that the gap between the valence band maximum of the adsorption system and the Fermi energy level will decrease in the range from −1.32 to −0.49 eV with increasing carbon chain length, which also verifies the enhanced adsorption effect for long chain alkanes on MoS_2. Therefore, for the selective removal of VOCs, the MoS_2 monolayer is a promising adsorbent, especially for the long chain VOC molecules.

3.4 Adsorption variability mechanism of VOCs on monolayer MoS_2

To further understand the variation trends in the adsorption mechanism of VOCs on monolayer MoS_2, we have calculated and shown the adsorption energies of 8 types of typical VOC species with different carbon chain lengths (C ≤ 8 atoms) in Fig. 8 and Table S1,† including alkanes, aromatic

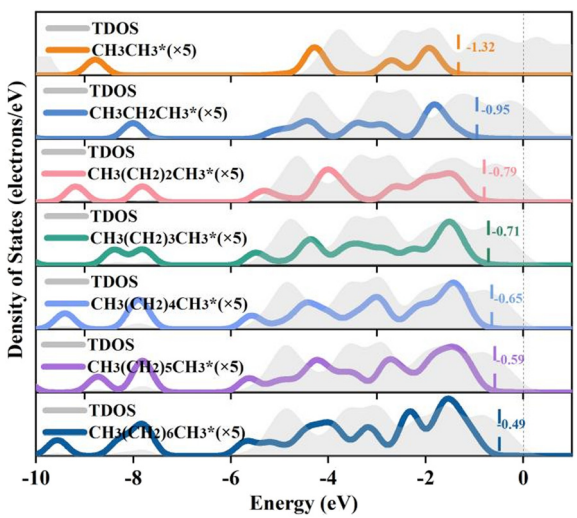

Fig. 7 The total and projected density of states for alkanes with varying carbon chain lengths adsorbed on monolayer MoS_2. The Fermi level is set to zero.

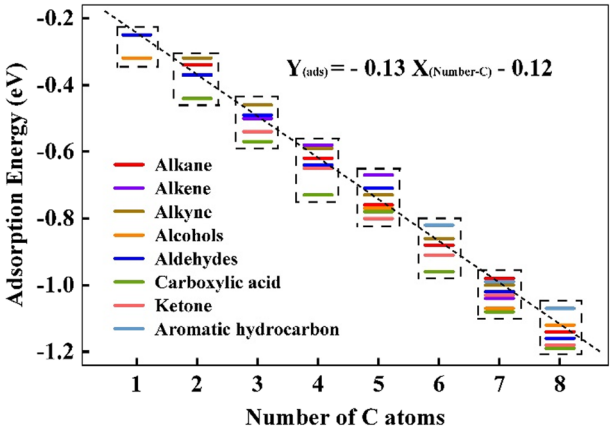

Fig. 8 Variation of adsorption energies for the eight types of typical VOCs (alkanes, alkenes, alkynes, alcohols, aldehydes, carboxylic acids, ketones and aromatic hydrocarbons) with the number of C atoms on monolayer MoS_2.

hydrocarbons, alkynes, aldehydes, ketones, alkene, alcohols and carboxylic acids. Except for aromatic hydrocarbons, all VOC molecular structures are straight carbon chains. The adsorption energy is defined by $E_{ads} = E_{system} - E_{MoS_2} - E_{VOCs}$, where E is the energy of the system at room temperature (298 K). The adsorption energy shows obvious regularity in Fig. 8, while it basically met the following order for different types of VOCs: alkanes < aromatic hydrocarbons < alkynes < aldehydes < ketones < alkenes < alcohols < carboxylic acids, with increasing carbon chain length. Furthermore, a fitting curve for the adsorption energy of all types of VOCs with different carbon chain lengths was predicted and drawn, which basically met the average regression line $Y = -0.13X - 0.12$, with X being the number of carbon atoms. The negative adsorption energy indicates that the adsorption process is exothermic. Among these VOCs, the formaldehyde possessed the minimum adsorption energy of −0.25 eV, which is still within the range of physical adsorption.[49] Overall, carboxylic acid had the highest adsorption energy under the same carbon chain length.

In addition to high sensitivity and selectivity, good reproduction and stability[50] are required for practically applied gas sensor materials in the removal of VOCs by adsorption technology. For the structure optimization of the stable configuration on MoS_2, the configuration of the MoS_2 layer was almost impervious with bond length and only a small disturbance in bond angle, which is within the allowable range of calculation, considering the difference calculation parameters. It is reported that[50] the 2H phase monolayer MoS_2 has excellent adsorption performance for different types of VOC molecules with a 1.9 eV band gap,[9] and its suitable band gap positions are widely used in the field of photocatalysis. Good adsorption characteristics are also a necessary prerequisite for photocatalysis.[4] Therefore, it is feasible to use MoS_2 as a good adsorbent for various types of VOC molecules.

For various types of VOCs, it is important to be able to selectively adsorb specific VOC species, which is also a key step in gas sensor detection. The basic principle is to convert signals such as gas composition and concentration into electrical signals, so as to realize the detection of gas types. The main electrical characteristics of the gas sensor include adsorption energy, charge transfer, electronic density of state, bandwidth and other parameters, which can be used to measure the performance of the gas sensor.[51] In the process of VOC removal, the adsorption site on the adsorbent can greatly affect the removal efficiency. Moreover, the adsorption configuration becomes more stable with lower free energy of the entire adsorption system, resulting in more VOC molecules that will be adsorbed on the limited catalyst surface. Single-layer MoS_2 is also used as the gas sensor materials for hexane, acetone and others VOC species. In addition, a recent article has confirmed that MoS_2 has a good response to gaseous VOCs.[52] Based on our calculations, it can be inferred that the monolayer MoS_2 exhibits a pronounced response to the aforementioned eight types of VOCs. Specifically, carboxylic acids demonstrate a high adsorption affinity for the monolayer MoS_2, whereas alkanes exhibit significantly lower adsorption tendencies. In addition, within the same category of VOCs, those with longer carbon chains are more readily adsorbed onto the MoS_2 surface compared to their shorter-chain counterparts (*cf.* Fig. 9).

4. Conclusions

In conclusion, we systematically investigated the adsorption mechanism of eight typical types of VOC molecules (including alkanes, alkenes, alkynes, alcohols, aldehydes, carboxylic acids, ketones and aromatic hydrocarbons) with 2–8 carbon chain lengths onto the MoS_2 monolayer by first-principle computations. The adsorption energy showed obvious regularity, while it basically met the following order for different types of VOCs: alkanes < aromatic hydrocarbons < alkynes < aldehydes < ketones < alkenes < alcohols < carboxylic acids, with the increase of carbon chain length. A fitting curve for the adsorption energy of all types of VOCs with different carbon chain length was drawn, wherein it essentially met the average regression line $Y = -0.13X - 0.12$. It demonstrated that the MoS_2 monolayer can be used as a very effective adsorbent for VOC molecules. This work explained the adsorption process of VOCs by MoS_2 in detail

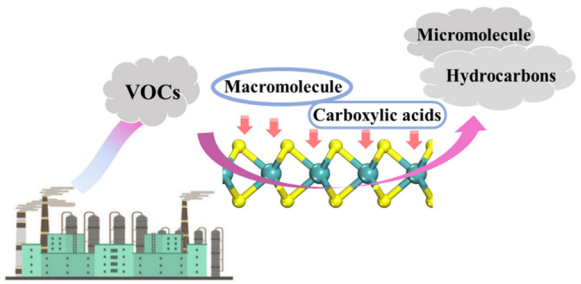

Fig. 9 Schematic of the adsorption diversity of different types of VOCs on the monolayer MoS_2.

from the aspect of the electronic structure, providing a comprehensive molecular understanding of the adsorption mechanism of eight types of VOCs and their derivatives with different carbon chain lengths in MoS_2. The adsorption effect of different VOCs on MoS_2 also showed a clear regular distribution, while the MoS_2 monolayer had a more noticeable removal effect of carboxylic acid organics due to the stronger charge transfer and adsorption energy of carboxylic acid organics.[53] The results show that it is feasible to use MoS_2 as a good adsorbent for various types of VOC adsorption and recovery in industrial production.

Data availability

The data supporting this article have been included as part of the ESI.†

Author contributions

Weina Zhao performed the conceptualization, and writing – original draft & editing; Jinlong Wang performed the modelling, theoretical calculation, and writing – original draft; Chang Shen performed the modelling and theoretical calculation; Bufan Xie performed the theoretical calculation and drawing; Guiying Li helped with the writing – review & editing; Taicheng An provided supervision, and contributed significantly to the manuscript preparation and review.

Conflicts of interest

There are no conflicts to declare.

Acknowledgements

This work was supported by the National Natural Science Foundation of China (22006023), Guangdong Provincial Key R&D Program (2022-GDUT-A0007), Natural Science Foundation of Guangdong Province (2019A1515010428) and the Guangzhou Science and Technology Project (202102020126).

Notes and references

1 Y. Gao, F. F. Yan, M. C. Ma, A. J. Ding, H. Liao, S. X. Wang, X. M. Wang, B. Zhao, W. J. Cai, H. Su, X. H. Yao and H. W. Gao, Unveiling the dipole synergic effect of biogenic and anthropogenic emissions on ozone concentrations, *Sci. Total Environ.*, 2022, **818**, 151722.

2 C. Holder, J. Hader, R. Avanasi, T. Hong, E. Carr, B. Mendez, J. Wignall, G. Glen, B. Guelden and Y. H. Wei, Evaluating potential human health risks from modeled inhalation exposures to volatile organic compounds emitted from oil and gas operations, *J. Air Waste Manage. Assoc.*, 2019, **69**, 1503–1524.

3 V. T. D. Hien, C. Lin, V. C. Thanh, N. T. K. Oanh, B. X. Thanh, C. E. Weng, C. S. Yuan and E. R. Rene, An overview of the development of vertical sampling technologies for ambient volatile organic compounds (VOCs), *J. Environ. Manage.*, 2019, **247**, 401–412.

4 L. K. Hoseini, R. J. Yengejeh, M. M. Rouzbehani and S. Sabzalipour, Health risk assessment of volatile organic compounds (VOCs) in a refinery in the southwest of Iran using SQRA method, *Public Health Front.*, 2022, **10**, 978354.

5 M. H. Yan, Y. B. Zhai, P. T. Shi, Y. J. Hu, H. J. Yang and H. J. Zhao, Emission of volatile organic compounds from new furniture products and its impact on human health, *Hum. Ecol. Risk Assess.*, 2019, **25**, 1886–1906.

6 W. Zhang, G. Li, H. Yin, K. Zhao, H. Zhao and T. An, Adsorption and desorption mechanism of aromatic VOCs onto porous carbon adsorbents for emission control and resource recovery: recent progress and challenges, *Environ. Sci.:Nano*, 2022, **9**, 81–104.

7 D. S. Alvim, L. V. Gatti, S. M. Correa, J. B. Chiquetto, C. D. Rossatti, A. Pretto, M. H. dos Santos, A. Yamazaki, J. P. Orlando and G. M. Santos, Main ozone-forming VOCs in the city of Sao Paulo: observations, modelling and impacts, *Air Qual., Atmos. Health*, 2017, **10**, 421–435.

8 S. Mousavinezhad, Y. Choi, A. Pouyaei, M. Ghahremanloo and D. L. Nelson, A comprehensive investigation of surface ozone pollution in China, 2015-2019: Separating the contributions from meteorology and precursor emissions, *Atmos. Res.*, 2021, **257**, 105599.

9 D. W. Ma, W. W. Ju, T. X. Li, G. Yang, C. Z. He, B. Y. Ma, Y. N. Tang, Z. S. Lu and Z. X. Yang, Formaldehyde molecule adsorption on the doped monolayer MoS_2: A first-principles study, *Appl. Surf. Sci.*, 2016, **371**, 180–188.

10 W. K. Pui, R. Yusoff and M. K. Aroua, A review on activated carbon adsorption for volatile organic compounds (VOCs), *Rev. Chem. Eng.*, 2019, **35**, 649–668.

11 Q. Y. Li, B. A. Liu and Z. M. Ao, Photocatalytic degradation of typical VOCs on sulfur-doped porous graphene, *Chin. Sci. Bull.*, 2022, **67**, 976–985.

12 Y. X. Wang, Y. Y. Zhang, X. J. Zhu, Y. Liu and Z. B. Wu, Fluorine-induced oxygen vacancies on TiO_2 nanosheets for photocatalytic indoor VOCs degradation, *Appl. Catal., B*, 2022, **316**, 121610.

13 K. Zhou, W. W. Ma, Z. Zeng, X. C. Ma, X. Xu, Y. Guo, H. L. Li and L. Q. Li, Experimental and DFT study on the adsorption of VOCs on activated carbon/metal oxides composites, *Chem. Eng. J.*, 2019, **372**, 1122–1133.

14 X. Y. Zhang, B. Gao, A. E. Creamer, C. C. Cao and Y. C. Li, Adsorption of VOCs onto engineered carbon materials: A review, *J. Hazard. Mater.*, 2017, **338**, 102–123.

15 H. B. Huang, G. Y. Liu, Y. J. Zhan, Y. Xu, H. X. Lu, H. L. Huang, Q. Y. Feng and M. Y. Wu, Photocatalytic Oxidation of Gaseous Benzene under VUV Irradiation over TiO_2/Zeolites Catalysts, *Catal. Today*, 2017, **281**, 649–655.

16 L. Zhu, D. Shen and K. H. Luo, A critical review on VOCs adsorption by different porous materials: Species, mechanisms and modification methods, *J. Hazard. Mater.*, 2020, **389**, 122102.

17 C. Yang, G. Miao, Y. Pi, Q. Xia, J. Wu, Z. Li and J. Xiao, Abatement of various types of VOCs by adsorption/catalytic oxidation: A review, *Chem. Eng. J.*, 2019, **370**, 1128–1153.
18 D. Adekoya, S. Zhang and M. Hankel, 1D/2D C(3)N(4)/Graphene Composite as a Preferred Anode Material for Lithium Ion Batteries: Importance of Heterostructure Design via DFT Computation, *ACS Appl. Mater. Interfaces*, 2020, **12**, 25875–25883.
19 K. Watanabe, T. Taniguchi and H. Kanda, Direct-bandgap properties and evidence for ultraviolet lasing of hexagonal boron nitride single crystal, *Nat. Mater.*, 2004, **3**, 404–409.
20 X. Deng, X. Liang, S.-P. Ng and C.-M. L. Wu, Adsorption of formaldehyde on transition metal doped monolayer MoS_2: A DFT study, *Appl. Surf. Sci.*, 2019, **484**, 1244–1252.
21 H. Detz and V. Butera, Insights into the mechanistic CO_2 conversion to methanol on single Ru atom anchored on MoS_2 monolayer, *Mol. Catal.*, 2023, **535**, 112878.
22 Y. Cong, W. Zhang, W. Ding, T. Zhang, Y. Zhang, N. Chi and Q. Wang, Fabrication of electrochemically-modified $BiVO_4$-MoS_2-Co_3O_4 composite film for bisphenol A degradation, *J. Environ. Sci.*, 2021, **102**, 341–351.
23 J. Wang, Q. Zhou, L. Xu, X. Gao and W. Zeng, Gas sensing mechanism of dissolved gases in transformer oil on Ag–MoS_2 monolayer: A DFT study, *Phys. E*, 2020, **118**, 113947.
24 S. Zhao, J. Xue and W. Kang, Gas adsorption on MoS_2 monolayer from first-principles calculations, *Chem. Phys. Lett.*, 2014, **595**, 35–42.
25 A. Shokri and N. Salami, Gas sensor based on MoS_2 monolayer, *Sens. Actuators, B*, 2016, **236**, 378–385.
26 V. Nagarajan and R. Chandiramouli, Adsorption studies of alcohol molecules on monolayer MoS_2 nanosheet—A first-principles insights, *Appl. Surf. Sci.*, 2017, **413**, 109–117.
27 X.-Q. Tian, L. Liu, X.-R. Wang, Y.-D. Wei, J. Gu, Y. Du and B. I. Yakobson, Engineering of the interactions of volatile organic compounds with MoS2, *J. Mater. Chem. C*, 2017, **5**, 1463–1470.
28 A. Abbasi, A. Abdelrasoul and J. J. Sardroodi, Adsorption of CO and NO molecules on Al, P and Si embedded MoS_2 nanosheets investigated by DFT calculations, *Adsorption*, 2019, **25**, 1001–1017.
29 Y. Liu, Z. Yang, L. Huang, W. Zeng and Q. Zhou, Anti-interference detection of mixed NOX via In_2O_3-based sensor array combining with neural network model at room temperature, *J. Hazard. Mater.*, 2024, **463**, 132857.
30 D. Lu, L. Huang, J. Zhang, W. Zeng and Q. Zhou, Pt decorated Janus WSSe monolayer: A gas-sensitive material candidate for SF6 decomposition gases based on the first-principles, *J. Environ. Chem. Eng.*, 2024, **12**, 112388.
31 B. Li, Q. Zhou, R. Peng, Y. Liao and W. Zeng, Adsorption of SF6 decomposition gases (H_2S, SO_2, SOF_2 and SO_2F_2) on Sc-doped MoS2 surface: A DFT study, *Appl. Surf. Sci.*, 2021, **549**, 149271.
32 X. Gui, Q. Zhou, S. Peng, L. Xu and W. Zeng, Adsorption behavior of Rh-doped MoS_2 monolayer towards SO_2, SOF_2, SO_2F_2 based on DFT study, *Phys. E*, 2020, **122**, 114224.
33 J. Wang, Q. Zhou, Z. Lu, Z. Wei and W. Zeng, Gas sensing performances and mechanism at atomic level of Au-MoS2 microspheres, *Appl. Surf. Sci.*, 2019, **490**, 124–136.
34 F. Chen, C. Hong, J. Jiang, Z. Zhang and Q. Zhou, A comparative DFT study on the adsorption properties of lithium batteries thermal runaway gases CO, CO_2, CH_4 and C_2H_4 on pristine and Au doped CdS monolayer, *Surf. Interfaces*, 2024, **46**, 104200.
35 C. Shen, Y. Chen and W. Zhao, Enhanced VOCs adsorption on Group VIII transition metal-doped MoS_2: A DFT study, *Chem. Phys.*, 2025, **589**, 112497.
36 B. Delley, From molecules to solids with the DMol3 approach, *J. Chem. Phys.*, 2000, **113**, 7756–7764.
37 Q. Li, L. Xu, K.-W. Luo, L.-L. Wang and X.-F. Li, SiC/MoS_2 layered heterostructures: Promising photocatalysts revealed by a first-principles study, *Mater. Chem. Phys.*, 2018, **216**, 64–71.
38 F. Ortmann, F. Bechstedt and W. G. Schmidt, Semiempirical van der Waals correction to the density functional description of solids and molecular structures, *Phys. Rev. B: Condens. Matter Mater. Phys.*, 2006, **73**, 205101.
39 F. Guo, J. Jia, D. Dai and H. Gao, The electronic properties and enhanced photocatalytic mechanism of TiO_2 hybridized with MoS_2 sheet, *Phys. E*, 2018, **97**, 31–37.
40 M. Kamruzzamana, J. A. Zapien, M. Rahman, R. Afrose, T. K. Anam, M. N. H. Liton, M. Al-Helal and M. K. R. Khan, Effects of p-type (Ag, Cu) dopant on the electronic, optical and photocatalytic properties of MoS_2, and impact on Au/Mo100-x-yAgxCuyS_2 performance, *J. Alloys Compd.*, 2021, **863**, 158366.
41 L. Huang, T. Li, W. Zeng and Q. Zhou, Two-dimensional Mo_3-TiS_2 monolayer hosting high moisture resistance and abundant surface-chemisorbed oxygen for effective detection of SF6 decomposition gases: Atomic-scale study, *Appl. Surf. Sci.*, 2024, **670**, 160651.
42 R. Peng, W. Zeng and Q. Zhou, Adsorption and gas sensing of dissolved gases in transformer oil onto Ru3-modified SnS_2: A DFT study, *Appl. Surf. Sci.*, 2023, **615**, 156445.
43 J. Zhang, T. Li, H. Zhang, Z. Huang, W. Zeng and Q. Zhou, Ni decorated ReS_2 monolayer as gas sensor or adsorbent for agricultural greenhouse gases NH_3, NO_2 and Cl_2: A DFT study, *Mater. Today Chem.*, 2024, **38**, 102114.
44 P. Raybaud, J. Hafner, G. Kresse and H. Toulhoat, Adsorption of thiophene on the catalytically active surface of MoS_2: An ab initio local-density-functional study, *Phys. Rev. Lett.*, 1998, **80**, 1481–1484.
45 K. Yang and B. Xing, Adsorption of Organic Compounds by Carbon Nanomaterials in Aqueous Phase: Polanyi Theory and Its Application, *Chem. Rev.*, 2010, **110**, 5989–6008.
46 A. Abbasi and J. J. Sardroodi, Adsorption of O_3, SO_2 and SO_3 gas molecules on MoS_2 monolayers: A computational investigation, *Appl. Surf. Sci.*, 2019, **469**, 781–791.
47 Y. Liu, Y. Dang, X. Feng, X. Chen and C. Yang, Promoting effect of Ni on the structure and electronic properties of NixMo(1−x)S_2 catalyst and benzene adsorption: A periodic DFT study, *Appl. Surf. Sci.*, 2019, **471**, 607–614.

48 M. Barzegar, M. Berahman and R. Asgari, First-principles study of molecule adsorption on Ni-decorated monolayer MoS_2, *J. Comput. Electron.*, 2019, **18**, 826–835.

49 V. Q. Bui, H. M. Le, Y. Kawazoe and Y. Kim, Adjusting band gap and charge transfer of organometallic complex adsorbed on MoS_2 monolayer using vertical electric-field: a first-principles investigation, *J. Phys.:Condens. Matter*, 2017, **29**, 015003.

50 W. Y. Chen, C. C. Yen, S. Xue, H. Wang and L. A. Stanciu, Surface Functionalization of Layered Molybdenum Disulfide for the Selective Detection of Volatile Organic Compounds at Room Temperature, *ACS Appl. Mater. Interfaces*, 2019, **11**, 34135–34143.

51 Y. Hosoya, Y. Itagaki, H. Aono and Y. Sadaoka, Ozone detection in air using $SmFeO_3$ gas sensor, *Sens. Actuators, B*, 2005, **108**, 198–201.

52 V. K. Tomer, R. Malik, V. Chaudhary, Y. K. Mishra, L. Kienle, R. Ahuja and L. Lin, Superior visible light photocatalysis and low-operating temperature VOCs sensor using cubic Ag(0)-MoS_2 loaded g-CN 3D porous hybrid, *Appl. Mater. Today*, 2019, **16**, 193–203.

53 J. Li, A. Listwan, J. Liang, F. Shi, K. Li and J. Jia, High proportion of 1 T phase MoS_2 prepared by a simple solvothermal method for high-efficiency electrocatalytic hydrogen evolution, *Chem. Eng. J.*, 2021, **422**, 130100.